2E11

NON-INTRUSIVE LASER BASED OPTICAL MEASUREMENT TECHNIQUES FOR REACTING AND NON-REACTING SUPERSONIC FLOWS

W. Gabler[1], F. Mayinger[2]

Lehrstuhl A für Thermodynamik, Technische Universität München
80290 Munich, Germany

Key Words: Flow Visualisation, Compressible Flows, Shock Waves, Turbulent Flows

ABSTRACT

In the framework of studies for airbreathing hypersonic propulsion systems, optical measurement techniques (shadowgraph imaging, Rayleigh scattering and laser induced fluorescence (LIF)) have been applied on the investigation of the mixing- and combustion process in supersonic hydrogen/air flames. The aim of the present contribution is to show the principles, applications and limitations of these diagnostic methods. The combined usage of these diagnostic techniques led to valuable data about the mixing and combustion process in supersonic combustion chambers, which are shown in this paper. Global qualitative information about the flow structure (shock wave pattern, reattachment length of free shear layers, visualisation of mixing jets and expansion waves) were taken from shadowgraphs. Rayleigh scattering and laser induced fluorescence (LIF) are adequate means for flow visualisation as well as for concentration and temperature measurements.

NOMENCLATURE

A_{12}	first Einstein coefficient
B_{12}	second Einstein coefficient
ER_{LIF}	intensity of the OH- fluorescence
f	focal length
L	length of the measuring volume
Ma	Mach number
m	mass flow of the fuel
N	number density of particles
n	refractive index
n_0	refractive index for gas at 273 K, 1 bar and a wavelength of 589,3 nm
r_m	density of the gas mixture
r_{0m}	density of the gas mixture at 273 K and 1 bar
I	intensity of the light beam
I_0	intensity of the incident light beam
I_r	intensity of Rayleigh scattered light
x	co-ordinate in the flow field
y	co-ordinate in the flow field
$(d\sigma/d\Omega)_{eff}$	effective differential scattering cross section
λ_0	wavelength of incident light
Ω	solid angle of collection

1. Introduction

A reduction of the combustor length due to shorter flame length and higher fuel efficiencies of supersonic propulsion systems can only be achieved via a better understanding of the complex fuel and air interactions during mixing and combustion. In this context, a detailed insight with high local and temporal resolution into thermo- and fluiddynamic processes is necessary. Since optical measurement techniques have high temporal and spatial resolution, they provide the capability to study the mixing and combustion process in supersonic flows, without perturbing the system under investigation. Flow measurements can be divided into two categories: visualisation of global flow characteristics, like shock pattern and shear layers by means of shadowgraph technique on one hand and detailed concentration and temperature measurements, using Rayleigh scattering and laser induced fluorescence on the other hand. This work intends to show the physical background, the special arrangement of the set-up of these measurement techniques, as well as selected representative results.

2. DIAGNOSTIC METHODS

2.1 Shadowgraph Technique

Shadowgraph technique is a comparatively simple qualitative technique to monitor features of the flow, like shock pattern, reattachment length of free shear layers, mixing jets and expansion waves. The physical background of this well-established technique is based on light deflection of a collimated laser beam (e.g. He-Ne-Laser, see fig. 1) crossing gradients of the index of refraction in a transparent probe (here supersonic flow in a combustion chamber equipped with windows).

[1] Scientific co-worker
[2] Professor and Head of the Institute

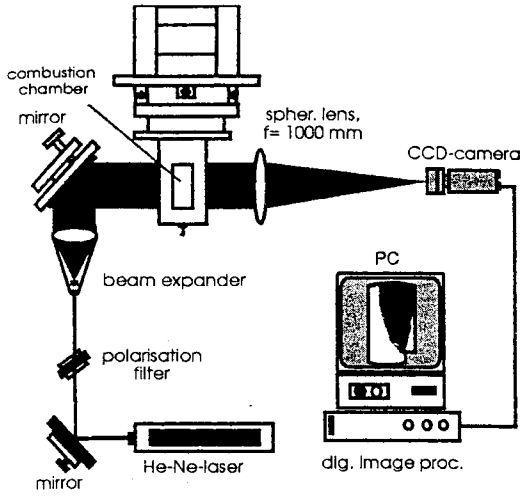

Fig 1. Optical set-up for shadowgraph imaging

The refractive index n depends on the density and the composition of the gases in the measuring object. The refractive index for a gas mixture can be obtained from equation 1.

$$n-1=(n_0-1)(\rho_m/\rho_{0m}) \qquad (1)$$

The light rays are projected onto an intensified CCD-camera after deviation (see fig 1). The relative intensity I of the light beam, detected by the camera is given by:

$$\frac{\Delta I}{I}=\frac{\partial^2\rho_m}{\partial x^2}+\frac{\partial^2\rho_m}{\partial y^2} \qquad (2)$$

In spite of this simple equation, a quantitative evaluation of shadowgraph images is extremely difficult, because a double integration of equation 2 is inclined to produce inaccurate results. In supersonic combustion chambers with gradients in concentration and temperature, a quantitative evaluation of shadowgraph images is impossible, since the refractive index n depends on the temperature/density and on the concentration of different gases in the measuring object. Hence, nothing can be said about the mixing rate or the concentration distribution. What's more, shadowgraph images have only poor spatial resolution in depth. Therefore, by means of shadowgraph technique only two dimensional structures can be resolved. For three dimensional problems, laser imaging methods, using two dimensional light sheets, have been employed (see Chap. 2.2 and 2.3).
Nevertheless, due to the high sensitivity of shadowgraph to density gradients, the shadowgraph technique is a useful tool to visualise shear layers, mixing jets, and shock waves in supersonic combustors.

Fig. 2 shows as an example a shadowgraph of a supersonic flow field. It exhibits the location of the oblique shock wave system, the mixing layer and the shear layer in the vicinity of a backward facing step in a supersonic combustion chamber. The Mach number Ma of the initial air flow is 2.1. Fuel is injected perpendicular to the air flow. Due to penetration of the injected fuel an oblique shock wave is generated in front of the fuel jet. This shock wave is reflected on the upper chamber wall and impinges onto the mixing shear layer downstream.

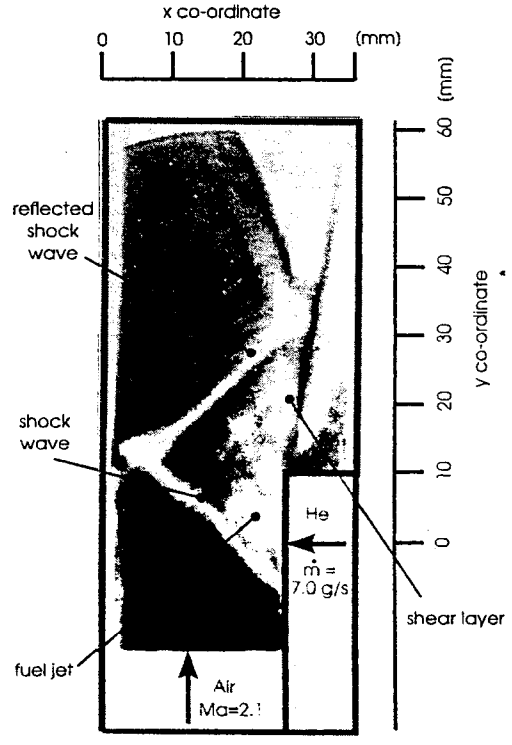

Fig. 2: Supersonic flow field with fuel injection (Ma = 2.1, m = 7,0 g/s)

2.2 Rayleigh Scattering

The Rayleigh effect is based on elastic scattering processes between incident photons and particles (atoms and molecules), which are smaller than the wavelength of the incident radiation. During the scattering process, the particles absorb photons of the incident light and are excited to a virtual quantum state (fig 3). Since this state is very unstable, the particles immediately return to its ground state emitting photons. According to the elastic property of the scattering process, the emitted light has the same wavelength as the incident light. Rayleigh scattering can be applied to conduct density or tempera-

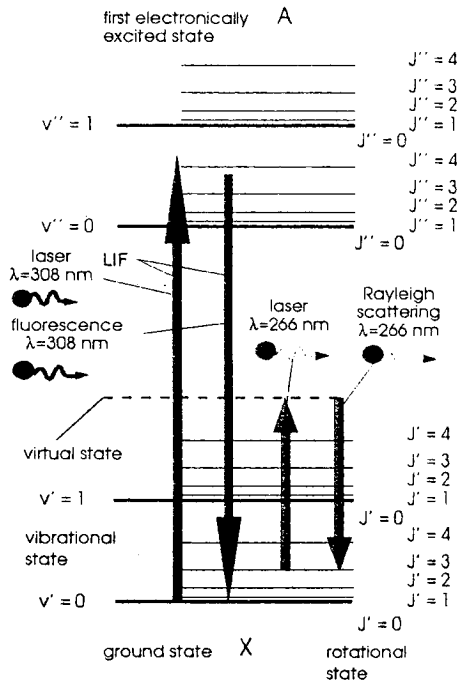

Fig. 3: Energy diagram for Rayleigh transition and laser induced fluorescence

ture measurements in gases and gaseous mixtures. Because of the relatively high intensity of the scattered light two dimensional measurements, using a laser-light-sheet, are possible. Fig. 4 shows a typical experimental set-up for planar Rayleigh measurements. The laser beam, coming from a Nd-YAG-laser with a wavelength of 266 nm and a pulse duration of 6 ns, is formed to a thin light sheet with a thickness of 0.3 mm and a height of 20 mm by a set of lenses. Normally, the lens set-up consists of a cylindrical lens (f=100 mm) followed by a spherical

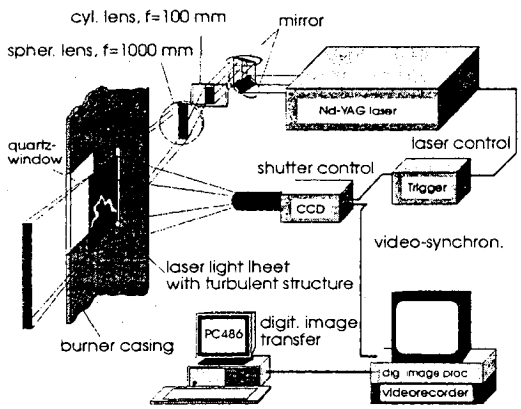

Fig. 4: Typical set-up for planar Rayleigh scattering measurements

convex lens with a long focal length (f = 1000 mm). The scattered light is captured perpendicular to the laser incident beam by a quartz glass objective and imaged onto the detector of a UV-intensivied CCD-camera. The obtained image is stored in grey scale values according to the intensity of emitted light.

The intensity of the Rayleigh scattered light is given by

$$I_r = I_0 \left(\frac{d\sigma}{d\Omega}\right)_{eff} \Omega L N \qquad (3)$$

According to equation 3, the intensity of the scattered light is in direct proportion to the number density N of the gas and the effective differential scattering cross section $(d\sigma/d\Omega)_{eff}$, which depends on the species undergoing the scattering process and the wavelength λ_0 of the incident radiation.

Since the differential scattering cross-section $(d\sigma/d\Omega)_{eff}$ is proportional to $1/\lambda_0^4$, the wavelength of the incident light should be as low as possible to gain higher signal intensities [1].

Except the effective differential scattering, cross-section $(d\sigma/d\Omega)_{eff}$ and the number density N, all factors in equation 3 can be calculated. The effective differential scattering cross-sections for several gases for an incident wavelength of 266 nm, taken from the literature [2], are summarised in tab. 1.

gas	scattering cross-section for λ_0 = 266 nm normalised to nitrogen
O_2	1.09
N_2	1
He	0.01
H_2	0.23

Tab. 1: differential scattering cross-sections for several gases for an incident wavelength of 266 nm [2]

For quantitative measurements in a system with gradients in concentration and density, like a non-reacting supersonic flow, it is necessary, that either the concentration or the density distribution in the object of measurement are known. Using Raman spectroscopy to determine the temperature distribution together with pressure measurements, the Rayleigh diagnostic system can be easily calibrated and on-line planar measurements of the concentration distribution can be carried out.

Figure 5 depicts the turbulent structure of the supersonic flow and the concentration distribution in the mixing jet. The mixing process of fuel and oxidiser is not influenced by chemical processes since helium was used as model gas instead of hydrogen. Due to the short laser

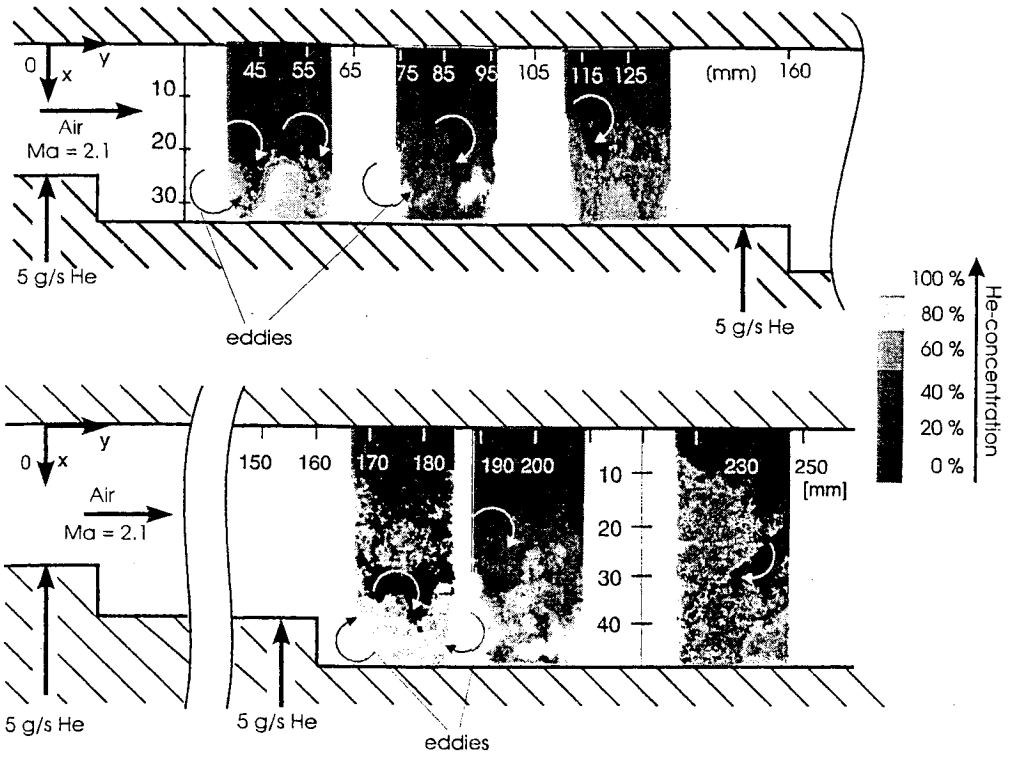

Fig. 5: Turbulent flow structure and concentration distribution in the mixing jet at Ma = 2.1 (m = 10 g/s)

pulse duration of 6 ns, even high transient turbulent flow structures are visualised. In this picture large scaled vortices, which are originated by the fuel injection and the flow around the rearward facing steps, can be observed. Comparing the images in the vicinity of the first rearward facing step with the pictures downstream of the second step, it can be seen that, turbulent structures are more spreaded and penetrate deeper into the surrounding air flow. Furthermore, downstream of the second step all turbulent structures consist of comustible mixtures. This indicate a strong increase in the mixing rate.

2.3 Laser Induced Fluorescence

Laser induced fluorescence (LIF) has its physical background in laser excitation, followed by natural fluorescence of molecules or atoms. A laser beam, which is tuned to a resonant wavelength of a regarded molecule or atom (O2, NO, OH, etc.) promotes a considerable number of them from the densely populated lower energy levels to the weakly populated excited state (see fig. 3). After an extremely short relaxation time of about (10^{-8} to 10^{-6} s), the molecules or atoms return to its original ground state by emitting a fluorescence light. Due to the large fluorescence intensities, the main field of application of LIF is the planar imaging of reacting flows [3,4,5].

In supersonic combustion chambers fired with hydrogen, LIF is applied to visualise OH-radicals in the reaction zone, which are interim products of the chemical reaction of hydrogen and oxidiser. These OH-radicals indicate the location and extension of the reaction zones. The laser optical set-up is approximately the same as for Rayleigh measurements, shown in figure 4. For laser induced fluorescence, a pulsed laser beam from a XeCl EXCIMER-laser at a wavelength of 308 nm and a duration of 17 ns is expanded into a sheet of light by means of a lens set-up, as shown in figure 4. Passing through the test-section, the light sheet excites (0,0)-band of the $A^2\Sigma \prod X^2\Pi$ system of the OH-radicals. The resulting OH fluorescence is monitored perpendicular to the laser sheet with a UV-intensified CCD-camera. The intensity of the obtained grey scale image is direct proportional to the number density N of OH-molecules in the flame front and indicates the local reaction rate of hydrogen and oxidiser. The intensity ER_{LIF} of the OH-fluorescence rate is as follows:

$$ER_{LIF} = NB_{12}I_0 \frac{A_{21}}{A_{21} + Q_{21}} \qquad (4)$$

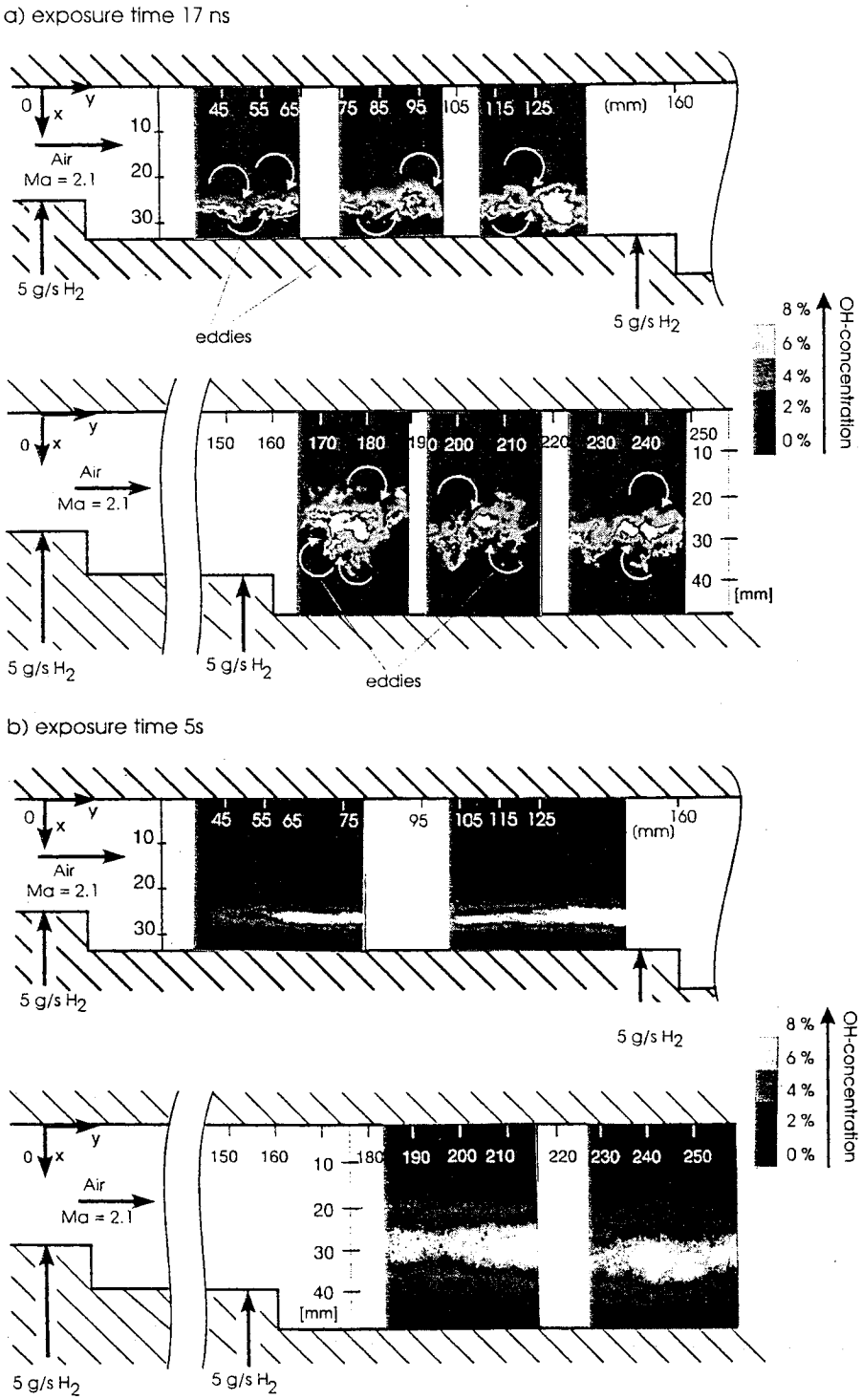

Fig. 6: Turbulent flame structure and OH-radical distribution in the vicinity of a rearward facing step (Ma = 2.1, m = 10 g/s)

The first and second Einstein coefficient A_{12} and B_{12} can be looked up in the literature [6]. Since the quench- and composition of gas under investigation, is unknown, only relative distributions of the OH-concentration can

Figure 6 shows a comparison of single shot images obtained with an exposure time of 17ns (a) and the corresponding images, averaged over multiple shots using an exposure time of 5s (b) in the vicinity of the first and second rearward facing step. The temporal resolution of the single shot measurements is determined by the duration of the laser pulse of 17 ns. Since the pulse is much shorter than any of the physical times associated with the reacting flow, the images show the instantaneous distribution of the OH-radical. Comparing the single shot images with the multiple shot pictures, it can be seen, that all large scaled eddies, created in the shear layer (see fig. 2), are within the corresponding mean flame profile. These eddies play a keyrole in reaction kinetics. Experiments have shown how the turbulent structure of the supersonic flow field has to be influenced by rearward facing steps and the geometry of the fuel injection system, to get more spreaded vortices with a higher rate of chemical reaction. Furthermore, both pictures illustrate that the stabilisation zone of the flame is located in the free shear layer (see fig. 2), which separates the mixing jet and the first recirculation zone. The highest velocity gradients are to be found in shear layers, correponding to a maximum turbulence enhancing the mixing process and the flame stabilisation.

The images concerning the cold mixing process (fig. 5) exhibit a combustible mixture in the first and second recirculation zone, whereas the corresponding pictures bout the reacting flow (fig. 6) show, that in these zones here is no chemical reaction. The explanation for this eature is, that in the reacting case the recirculation zone s filled up with hot exhaust gases. which enable the lame stabilisation by transporting energy to the ignition oint of the flame. The amount of the transported energy an be influenced by the step height. Using this mechaism it is possible to stabilise the flame at all operating onditions.

Comparing the outer border of the flame with the inner order (fig 6 a), it can be seen, that on the supersonic oundary the flame is influenced by fine scaled vortices, hereas on the subsonic boundary the flame is affected y large scale vortices. Due to large scaled vortices, duced by the second injection and the flow around the cond step, the rate of chemical reaction increases. On e top, the flame penetrates deeper into the surrounding r flow after the second rearward facing step.

3. Concluding Remarks

The investigations in reacting and non-reacting supernic flows presented in this paper show, that nontrusive laser based optical measurement techniques are lequate to reveal the structure of supersonic flows, as ell as the turbulent structure of supersonic reaction nes. Rayleigh scattering images provide even quantitive data about the mixing rate and the fuel distribution in supersonic combustion chambers. Although shadowgraph imaging is a qualitative measurement technique only, it provides useful data about the location of shock waves, expansion waves and shear layers. This technique is applied in order to select key locations in a supersonic flow field for more quantitative optical measurements, like Rayleigh scattering and laser induced fluorescence. Due to this, costly quantitative measurements can be avoided.

4. Acknowledgement

The authors would like to thank the Deutsche Forschungsgemeinschaft (DFG) for support of this research work under contract „Sonderforschungsbereich 255, Transatmosphärische Flugsysteme".

5. References

1. Mayinger F. (Ed.): Optical Measurement Techniques; Springer, New York, 1994

2. Landolt Börnstein: Zahlenwerte und Funktionen, Band II, 6. Auflage, Springer, Berlin, 1968

3. Haibel M., Mayinger F. and Strube G.: Application of non-intrusive diagnostic methodes to sub- and supersonic hydrogen/air flames, Proc. of the 3rd International Symposium on special topics in chemical propulsion, pp. 109-112. The Pennsylvania State University, University Park, Pa, 1993.

4. Mayinger F., Gabler W.: Spectroscopic Techniques for Ram Combustors, Proc. of the 2nd Space Course on Low Earth Orbit Transportation, Vol. 1 Munich, 1993.

5. Mayinger F.: Modern electronics in image-processing and physical modelling - A new challenge for optical techniques. Invited key note lecture, Proc. of the 10th Int. Heat Transfer Conference, Brighton, UK, Aug. 14-18, 1994, Eds.: Hewitt, G. F. et al. Vol. 1, pp. 61-79.

6. Huber, K.P., Herzberg, G.: Constants of Diatomic Molecules, van Nostrand, New York, 1979